Stellar/inertial integrated guidance for responsive launch vehicles

Zhang Hongbo *, Zheng Wei, Tang Guojian

College of Aerospace and Material Engineering, National University of Defense Technology, Changsha 410073, PR China

A B S T R A C T

Responsive space-lift is a new trend in space launches. It requires the guidance system of the launch vehicle to be easily prepared, precise, robust, and adaptive. The stellar/inertial integrated guidance system, which combines two distinct types of navigation data, has been successfully used for submarine-launched ballistic missiles. This paper focuses on its application for responsive launch vehicles. Only the prelaunch positioning and orientation errors are considered in order to provide a simple illustration of the basic principles, which can be conveniently generalized to practical launch activities with a well-developed optimum correction method. Error transition and measurement equations are constructed and two injection error correction schemes are proposed. Because the integrated guidance accuracy varies with regard to the stellar direction, an analytical method is addressed to determine the optimal navigation star. Finally, numerical studies are conducted and the results verify the integrated guidance policy. Stellar/inertial integrated guidance can simplify prelaunch preparation and improve the orbital injection accuracy. Thus, it provides an alternative that does not rely on man-made signals for responsive launch vehicles.

© 2011 Elsevier Masson SAS. All rights reserved.

1. Introduction

Over half a century of spaceflight, the activity of entering space is no longer astonishing. However, a reliable space launch requires exhaustive prelaunch preparation, which is time-consuming and costly work. Consequently, responsive space-lift has become a new trend in spaceflight [23,16]. The objectives of responsive space-lift include low launch cost, easy preparation, and convenient operation, which could make space launches a daily activity. Thus, guidance systems of launch vehicles need to be easily prepared, precise, robust, and adaptive.

Many guidance approaches have been investigated since the 1960s, all of which need to measure the real-time motion states of the vehicle to validate convergence and accuracy [10,8,25,12]. The most common implementation is the inertial navigation system (INS). However, inertial components (the gyroscopes and accelerometers) used in an INS have some unavoidable errors with stochastic properties. For vehicles with short flight times, such errors might be acceptable. For long-time duration missions, these errors tend to increase over time with unbounded position error growth. Thus, for precision guidance, the INS has to be augmented with external aids, among which the most extensively and successfully used is the Global Positioning System (GPS) [17,4,13]. Although GPS can offer highly accurate position information at very low cost, the likelihood that GPS may be denied to the user owing to interference or intentional jamming is of great concern and

thus motivates the investigation of alternatives. Typical aid devices include a vision sensor [24], magnetometer [11], gravimeter [19], and star sensor [20,1,18,7]. In the case of employing a star sensor, a Kalman filter has been used to combine stellar observations with INS outputs to enhance the navigation performance [20,1,18, 7]. This paper proposes another data fusion method for the ascending guidance in which the star-observing window is so short that no filter can be used.

The stellar/inertial integrated system is a simple and effective guidance implementation which has been successfully used for submarine-launched ballistic missiles. The stellar-updated inertial guidance system incorporates gyroscopes, accelerometers, and a star sensor in an inertially fixed stable element that mounted in a four-axis or five-axis servo-stabilized gimbal system (called inertial platform herein) [14]. Prior to launch, the star sensor is pointed in a computed direction through a leveling and alignment procedure, and the attitude is maintained during launch. At the end of the boost stage, prior to final cutoff, the star sensor carries out star observation. The output is used to compute the target impact error of the trajectory, and an appropriate velocity increment is made to reduce the predicted error to zero [15,6]. Thus, the stellar/inertial guidance system can reduce dependence on prelaunch preparation, enhance performance of inertial navigation, and improve guidance accuracy, all of which are in accordance with the requirements of responsive space-lift [23]. Although it has not been adopted by traditional launch vehicles mainly owing to a lower guidance accuracy requirement compared with that of ballistic missiles, it is a suitable guidance solution for responsive launch vehicles.

---

* Corresponding author.
E-mail address: laugh_talking@163.com (H. Zhang).

The fundamental of the guidance system is that observed stellar vector is used to determine misalignment angles of the inertial platform, from which guidance errors are estimated and corrected. Therefore, the procedure is basically a problem of attitude determination through vector observation. This kind of problem was first addressed and investigated by Wahba in the 1960s [21], and many algorithms have been developed since then [2,9,5]. Most require two observed vectors to achieve convergence, but some function well with a long-term observation of one vector [22]. Similarly, according to the number of vectors being measured, stellar/inertial integrated guidance systems can be categorized as single-star and double-star schemes. The difference is that impact point downrange and cross-range deviations can directly relate to the outputs of star sensor and there is no need to determine the attitude of the inertial platform. For there are only two accuracy indices, the single-star scheme can theoretically achieve the same accuracy as the double-star scheme by observing a specific vector, which is called the optimal stellar direction. For the launch vehicle guidance system, there are more than two accuracy indices, and that results in differences between the two schemes. In spite of that, the structural configuration of gimbals system and the correction procedure of orbital injection errors in the single-star scheme are simpler and more feasible, and thus, this paper explores the fundamentals and applications of the single-star scheme rather than those of the double-star scheme.

During a practical space launch, misalignment angles are introduced by many uncertainties, including prelaunch positioning and orientation errors, initial alignment and leveling errors, and inertia component errors. The stellar vector measurement cannot distinguish these errors into classes, and thus, a synthetic correction based on optimum estimation theory is required, supposing that the error distributions are known [15,6]. Because the optimum correction method has been well developed, for the sake of simple illustration, only prelaunch positioning and orientation errors are taken into account in this paper. It is also assumed that a five-axis servo-stabilized gimbal system is adopted so that the optical axis of the star sensor can aim at an arbitrary navigation star [6]. Undoubtedly, a strap-down star sensor has some virtues over the gimbal system. We adopt the servo-stabilized star tracker mainly for its maturity in application, and the principle of the stellar/inertial integrated guidance using a strap-down star sensor is almost the same with that studied in our paper.

The paper is organized as follows. In Section 2, error transition and measurement equations are derived and two orbital injection error correction schemes are proposed. An analytical method to determine the optimal stellar direction is presented in Section 3, and in Section 4, numerical studies are conducted to validate the foregoing conclusion.

2. Integrated guidance modeling

2.1. Error transition equation

Prelaunch positioning errors can be represented by orthogonal coordinate errors Δx_0, Δy_0, and Δz_0 in the geocentric fixed frame, or the longitude error $\Delta \lambda_0$, geographic latitude error ΔB_0, and altitude error ΔH_0 [3]. Using spherical triangle equations, we easily obtain the relationship between the two groups of errors

$$
\begin{bmatrix} \Delta x_0 \\ \Delta y_0 \\ \Delta z_0 \end{bmatrix} = \begin{bmatrix} (N+H_0)\cos B_0 \sin A_0 & (N+H_0)\cos A_0 & 0 \\ 0 & 0 & 1 \\ (N+H_0)\cos B_0 \cos A_0 & -(N+H_0)\sin A_0 & 0 \end{bmatrix} \\ \times \begin{bmatrix} \Delta \lambda_0 \\ \Delta B_0 \\ \Delta H_0 \end{bmatrix}, \tag{1}
$$

where A_0, B_0, N, and H_0 are the launch azimuth, geographic latitude, radius of the prime vertical, and altitude, respectively. Because the altitude error does not affect the inertial platform alignment and leveling, it cannot be modified through stellar measurement. Consequently, only $\Delta \lambda_0$, ΔB_0, and ΔA_0 (the launch azimuth error, representing the prelaunch orientation error) are considered in the following discussion.

Deviations of the motion states induced by the positioning and orientation errors can be divided into two parts: the initial errors of navigation computation and the integral errors brought by the misalignment between the inertial platform frame P and the launch point inertial frame I. The axes of the coordinate system P coincide with the gimbal axes [6]. The x axis of frame I is oriented along the range, and the z axis is perpendicular to the local horizontal plane. For the former part of the deviations, the initial position error is

$$
\Delta \mathbf{r}(t_0) = \begin{bmatrix} 0 & -(N+H_0) \\ 0 & 0 \\ (N+H_0) & 0 \end{bmatrix} \\ \times \begin{bmatrix} \cos A_0 \cos B_0 & -\sin A_0 \\ -\sin A_0 \cos B_0 & -\cos A_0 \end{bmatrix} \cdot \begin{bmatrix} \Delta \lambda_0 \\ \Delta B_0 \end{bmatrix} \tag{2}
$$

and the initial velocity error is

$$
\Delta \mathbf{v}(t_0) = \boldsymbol{\omega}_{e\times} \cdot \Delta \mathbf{r}(t_0), \tag{3}
$$

where $\boldsymbol{\omega}_{e\times}$ is the anti-symmetric matrix of the Earth spin angular velocity $\boldsymbol{\omega}_e$. The definition of $\boldsymbol{\omega}_{e\times}$ is

$$
\boldsymbol{\omega}_{e\times} = \begin{bmatrix} 0 & -\omega_{ez} & \omega_{ey} \\ \omega_{ez} & 0 & -\omega_{ex} \\ -\omega_{ey} & \omega_{ex} & 0 \end{bmatrix}. \tag{4}
$$

The integral errors can be described in terms of the three misalignment angles α_x, α_y, and α_z. Suppose that frame I successively rotates about the three axes with angles α_x, α_y, and α_z to coincide with frame P. With first-order approximation, the direction cosine matrix for transformation between the two frames is expressed as

$$
\mathbf{C}_P^I = \begin{bmatrix} 1 & -\alpha_z & \alpha_y \\ \alpha_z & 1 & -\alpha_x \\ -\alpha_y & \alpha_x & 1 \end{bmatrix}. \tag{5}
$$

The direction cosine matrix for transformation between the geocentric inertial frame E and frame I is

$$
\mathbf{C}_E^I = \mathbf{M}_2\big[-(90°+A_0)\big] \cdot \mathbf{M}_1[B_0] \cdot \mathbf{M}_3\big[-(90°-\lambda_0)\big], \tag{6}
$$

where $\mathbf{M}_i$ $(i=1,2,3)$ are elementary rotation matrices [3]. Furthermore, because the inertial platform is aligned and leveled at the actual launch point, taking no account of the alignment and leveling errors, we obtain the direction cosine matrix for transformation between frame P and frame E

$$
\mathbf{C}_E^P = \mathbf{M}_2\big[-(90°+A_0+\Delta A_0)\big] \cdot \mathbf{M}_1[B_0+\Delta B_0] \\ \times \mathbf{M}_3\big[-(90°-\lambda_0-\Delta \lambda_0)\big]. \tag{7}
$$

Similarly, with first-order approximation, we can obtain another expression for the matrix $\mathbf{C}_P^I$ by multiplying Eqs. (6) and (7)

$$
\mathbf{C}_P^I = \mathbf{C}_E^I \cdot \mathbf{C}_P^E \\ = \begin{bmatrix} 1 & \begin{array}{c} \Delta B_0 \cos A_0 \\ + \Delta \lambda_0 \sin A_0 \cos B_0 \end{array} & \Delta \lambda_0 \sin B_0 - \Delta A_0 \\ \begin{array}{c} -(\Delta B_0 \cos A_0 \\ + \Delta \lambda_0 \sin A_0 \cos B_0) \end{array} & 1 & \begin{array}{c} \Delta B_0 \sin A_0 \\ - \Delta \lambda_0 \cos B_0 \cos A_0 \end{array} \\ -(\Delta \lambda_0 \sin B_0 - \Delta A_0) & \begin{array}{c} -(\Delta B_0 \sin A_0 \\ - \Delta \lambda_0 \cos B_0 \cos A_0) \end{array} & 1 \end{bmatrix}. \tag{8}
$$

Fig. 1. Stellar vector in the inertial frame.
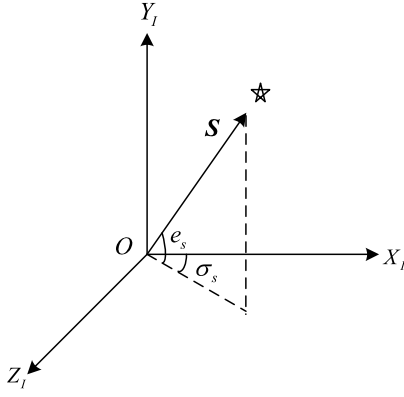

Fig. 2. Relationship between the star sensor body frame and the inertial platform frame.

Comparing Eq. (5) with Eq. (8), we find the relations between the misalignment angles and the positioning and orientation errors are

$$\boldsymbol{\alpha} = \begin{bmatrix} \alpha_x \\ \alpha_y \\ \alpha_z \end{bmatrix} = \begin{bmatrix} 0 & -\sin A_0 & \cos A_0 \cos B_0 \\ -1 & 0 & \sin B_0 \\ 0 & -\cos A_0 & -\cos B_0 \sin A_0 \end{bmatrix} \begin{bmatrix} \Delta A_0 \\ \Delta B_0 \\ \Delta \lambda_0 \end{bmatrix}$$
$$\triangleq \boldsymbol{P} \cdot \boldsymbol{\Delta}. \tag{9}$$

The matrix $\boldsymbol{P}$ is invertible when $B \neq 90°$; hence, generally $\boldsymbol{\alpha}$ uniquely corresponds to $\boldsymbol{\Delta}$. In other words, $\boldsymbol{\Delta}$ can be uniquely determined by measuring $\boldsymbol{\alpha}$.

According to the derivation above, the relationship between the integral errors and $\boldsymbol{\Delta}$ can be derived, although the expression is rather complicated. If we define $\boldsymbol{R}_k$ and $\boldsymbol{V}_k$ to be the vehicle position and velocity vectors when the star alignment is carried out, then expressions of the motion state deviations in terms of the positioning and orientation errors can be derived. They are expressed in a compact form as

$$\begin{bmatrix} \Delta \boldsymbol{R}_k \\ \Delta \boldsymbol{V}_k \end{bmatrix} = \begin{bmatrix} \partial \boldsymbol{R}_k / \partial A_0 & \partial \boldsymbol{R}_k / \partial B_0 & \partial \boldsymbol{R}_k / \partial \lambda_0 \\ \partial \boldsymbol{V}_k / \partial A_0 & \partial \boldsymbol{V}_k / \partial B_0 & \partial \boldsymbol{V}_k / \partial \lambda_0 \end{bmatrix} \begin{bmatrix} \Delta A_0 \\ \Delta B_0 \\ \Delta \lambda_0 \end{bmatrix}$$
$$\triangleq \boldsymbol{C} \cdot \boldsymbol{\Delta}. \tag{10}$$

The matrix $\boldsymbol{C}$ can be computed in advance for that particular position.

2.2. Measurement equation

We denote the elevation angle and azimuth angle of the stellar direction unit vector $\boldsymbol{S}$ in the frame I by e_s and σ_s, as shown in Fig. 1. The elevation angle is measured upward, while the azimuth angle is measured clockwise. Thus, vector $\boldsymbol{S}$ in frame I can be described as

$$\boldsymbol{S}_I = \begin{bmatrix} \cos e_s \cos \sigma_s & \sin e_s & \cos e_s \sin \sigma_s \end{bmatrix}^T. \tag{11}$$

To point to the navigation star, the star sensor body frame B rotates with regard to frame P, under the assumption that frame P coincides with frame I after alignment and leveling. Thus, frame P firstly rotates about the y axis by $-\sigma_s$ and then about the z axis by e_s to coincide with frame B, as shown in Fig. 2. The direction cosine matrix for the two frames is then derived as

$$\boldsymbol{C}_P^B = \boldsymbol{M}_3(e_s) \boldsymbol{M}_2(-\sigma_s)$$
$$= \begin{bmatrix} \cos e_s \cos \sigma_s & \sin e_s & \cos e_s \sin \sigma_s \\ -\sin e_s \cos \sigma_s & \cos e_s & -\sin e_s \sin \sigma_s \\ -\sin \sigma_s & 0 & \cos \sigma_s \end{bmatrix}. \tag{12}$$
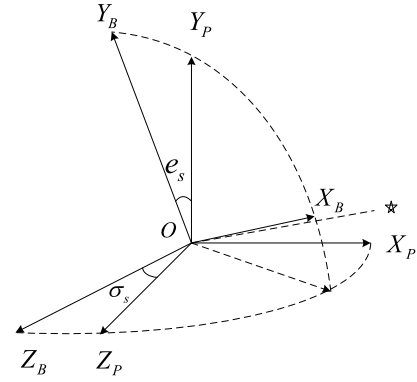
Since the optical axis OX_B is nearly collinear with the stellar direction vector, it is reasonable to assume that the cosine value of the included angle is 1. If the outputs of the star sensor are ξ and η, then vector $\boldsymbol{S}$ in frame B can be expressed as

$$\boldsymbol{S}_B = \begin{bmatrix} 1 & -\xi & -\eta \end{bmatrix}^T. \tag{13}$$

Therefore, the expression of vector $\boldsymbol{S}$ in frame P is

$$\boldsymbol{S}_P = \boldsymbol{C}_B^P \boldsymbol{S}_B. \tag{14}$$

According to the transfer relationship between coordinate systems, we obtain another expression of vector $\boldsymbol{S}$ in frame B

$$\boldsymbol{S}_B = \boldsymbol{C}_P^B \cdot \boldsymbol{C}_I^P \cdot \boldsymbol{S}_I. \tag{15}$$

Inserting the expressions of the related matrices and vectors into the preceding equation, the measurement equation is obtained as

$$\begin{bmatrix} \xi \\ \eta \end{bmatrix} = \begin{bmatrix} -\sin \sigma_s & 0 & \cos \sigma_s \\ \sin e_s \cos \sigma_s & -\cos e_s & \sin e_s \sin \sigma_s \end{bmatrix} \begin{bmatrix} \alpha_x \\ \alpha_y \\ \alpha_z \end{bmatrix}$$
$$\triangleq \begin{bmatrix} \boldsymbol{h}_1^T \\ \boldsymbol{h}_2^T \end{bmatrix} \boldsymbol{\alpha} \triangleq \boldsymbol{H} \boldsymbol{\alpha}. \tag{16}$$

Vector $\boldsymbol{w} = [\xi, \eta]^T$ is adopted to denote the outputs of the star sensor in the following.

2.3. Correction of orbit-injection error

When launching a satellite, six orbital element constraints are usually specified in order to accomplish scheduled tasks. The expected right ascension of ascending node is generally obtained by choosing launch window, while the true anomaly is obtained by in-orbit phasing. Constraints on the other four orbital elements, namely semi-major axis a, eccentricity e, orbital inclination i, and argument of perigee ω, usually hold by iterating launch program. Sometimes another four parameters, usually the geocentric distance r_k, magnitude of velocity v_k, flight path angle Θ_k, and orbital inclination i, are used as the iterating variables instead. The single-star scheme has only two measurements. Although some newly developed filtering algorithms can get the three attitude angles, the procedure of star alignment takes only a few minutes within which no filter could converge. Thus, to achieve optimal accuracy, two of the four iterating variables should be selected. The double-star scheme is capable of determining the three misalignment angles of the inertial platform, and hence all four parameters can be corrected, resulting in more promising accuracy. However, noticing that only three control variables (direction of thrust vector and the time of cutoff) are available during the correction, if

four injection parameters are corrected simultaneously, an optimal control algorithm should be employed to reach a satisfying result. For the correction duration is not long, simulations show that the convergence of the guidance algorithm is unstable. If only two parameters are corrected, the known and simple velocity-to-gain guidance algorithm can be used with reliable convergence. Furthermore, the structural configuration of a gimbal system containing two star sensors is much more complicated. Therefore, the single-star scheme is recommended and investigated in this paper.

A number of combinations of two members of the iterating variables can be chosen as correction parameters, among which two schemes are suggested in consideration of the importance of injection requirements. One is the semi-major axis a and orbital inclination i, and the other is the flight path angle Θ_k and orbital inclination i. It is known that a is a scalar that represents the orbital energy, while the measurements of the star sensor indicate the inertial platform drift, which somewhat is a vector. Thus, we deduce that the integrated system may not obviously improve the accuracy of a. Contrarily, Θ_k and i both imply information of the orientation, and in a manner can be respectively analogized to the longitudinal range and lateral range of ballistic missiles. Thus, a distinct correction effect can be expected. Although the correction difference between the parameters vanishes when only the positioning and orientation errors are taken into account, the deduction is verified by numerical simulations (results not presented here) when all the related errors that affect the misalignment angles are involved.

Partial derivatives of the correction parameters with respect to the motion states are derived as follows. We first define the direction cosine matrix for transformation between the frame I and the launch point equatorial inertial frame E_L (with the x axis pointing toward the intersection of the equator and the meridian of the launch point) as

$$C_I^{E_L} = M_3\left[\frac{\pi}{2}\right] \cdot M_1[-B_0] \cdot M_2\left[\frac{\pi}{2} + A_0\right]. \tag{17}$$

If we denote the geocentric vector of the launch point by r_L, it is clear that the position and velocity vectors before star alignment in frame E_L are

$$\begin{cases} R_{Ek} = C_I^{E_L}(R_k + r_L), \\ V_{Ek} = C_I^{E_L} V_k. \end{cases} \tag{18}$$

The angular momentum is

$$h_k = R_{Ek} \times V_{Ek}. \tag{19}$$

According to the relations between the orbital elements and motion states [3], one has

$$a = \frac{R_{Ek}}{2 - \upsilon_k}, \tag{20}$$

$$i = \cos^{-1}\frac{h_{kz}}{h_k}, \quad \text{and} \tag{21}$$

$$\Theta_k = \sin^{-1}\frac{R_{Ek} \cdot V_{Ek}}{R_{Ek} V_{Ek}}, \tag{22}$$

where $\upsilon_k = R_{Ek} V_{Ek}^2/\mu$ and μ is the gravitational constant of the Earth.

Taking the derivative of Eq. (20), the partial derivative of a with respect to the cutoff states is obtained as

$$\begin{cases} \dfrac{\partial a}{\partial R_{Ek}} = \dfrac{2\mu^2}{(R_{Ek} V_{Ek}^2 - 2\mu)^2} \cdot \dfrac{R_{Ek}}{R_{Ek}}, \\ \dfrac{\partial a}{\partial V_{Ek}} = \dfrac{2\mu R_{Ek}^2 V_{Ek}}{(R_{Ek} V_{Ek}^2 - 2\mu)^2} \cdot \dfrac{V_{Ek}}{V_{Ek}}. \end{cases} \tag{23}$$

Similarly, by taking derivatives of Eqs. (21) and (22), the partial derivatives of i and Θ_k with respect to the cutoff states are derived as

$$\begin{cases} \dfrac{\partial i}{\partial R_{Ek}} = -\dfrac{1}{h_k^2\sqrt{h_{kx}^2 + h_{ky}^2}}\left[h_k^2\begin{bmatrix} V_{Eky} \\ -V_{Ekx} \\ 0 \end{bmatrix} + h_{kz}(h_k \times V_{Ek}) \right], \\ \dfrac{\partial i}{\partial V_{Ek}} = -\dfrac{1}{h_k^2\sqrt{h_{kx}^2 + h_{ky}^2}}\left[h_k^2\begin{bmatrix} -R_{Eky} \\ R_{Ekx} \\ 0 \end{bmatrix} - h_{kz}(h_k \times R_{Ek}) \right] \end{cases} \tag{24}$$

and

$$\begin{cases} \dfrac{\partial \Theta_k}{\partial R_{Ek}} = \dfrac{V_{Ek}}{R_{Ek} V_{Ek}\sqrt{(R_{Ek}V_{Ek})^2 - (R_{Ek} \cdot V_{Ek})^2}} \\ \qquad \times \left[R_{Ek}V_{Ek} - (R_{Ek} \cdot V_{Ek})\dfrac{R_{Ek}}{R_{Ek}} \right], \\ \dfrac{\partial \Theta_k}{\partial V_{Ek}} = \dfrac{R_{Ek}}{R_{Ek} V_{Ek}\sqrt{(R_{Ek}V_{Ek})^2 - (R_{Ek} \cdot V_{Ek})^2}} \\ \qquad \times \left[V_{Ek}R_{Ek} - (R_{Ek} \cdot V_{Ek})\dfrac{V_{Ek}}{V_{Ek}} \right]. \end{cases} \tag{25}$$

We denote the correction parameters of the two schemes proposed above as m_1 and m_2. Combining Eq. (18) with Eqs. (23)–(25), we obtain the partial derivatives expressed in frame I

$$\begin{cases} \dfrac{\partial m_i}{\partial R_k} = C_I^{E_L} \cdot \dfrac{\partial m_i}{\partial R_{Ek}}, \\ \dfrac{\partial m_i}{\partial V_k} = C_I^{E_L} \cdot \dfrac{\partial m_i}{\partial V_{Ek}}, \end{cases} \quad i = 1, 2. \tag{26}$$

From Eqs. (10) and (26), the relationship between the motion state deviations and the initial errors is obtained as

$$\begin{aligned} \begin{bmatrix} \Delta m_1 \\ \Delta m_2 \end{bmatrix} &= \begin{bmatrix} (\frac{\partial m_1}{\partial V_k})^T & (\frac{\partial m_1}{\partial R_k})^T \\ (\frac{\partial m_2}{\partial V_k})^T & (\frac{\partial m_2}{\partial R_k})^T \end{bmatrix} \cdot C \cdot \Delta \triangleq \begin{bmatrix} \frac{\partial m_1}{\partial \Delta^T} \\ \frac{\partial m_2}{\partial \Delta^T} \end{bmatrix} \cdot \Delta \\ &\triangleq \begin{bmatrix} C_{m_1}^{\Delta} \\ C_{m_2}^{\Delta} \end{bmatrix} \cdot \Delta. \end{aligned} \tag{27}$$

From Eq. (9), we obtain $\Delta = P^{-1} \cdot \alpha = D \cdot \alpha$. Inserting the expression into the foregoing equation, we express the injection errors in terms of the misalignment angles in a compact form as

$$\begin{aligned} \begin{bmatrix} \Delta m_1 \\ \Delta m_2 \end{bmatrix} &= \begin{bmatrix} \partial m_1/\partial \alpha_x & \partial m_1/\partial \alpha_y & \partial m_1/\partial \alpha_z \\ \partial m_2/\partial \alpha_x & \partial m_2/\partial \alpha_y & \partial m_2/\partial \alpha_z \end{bmatrix} \begin{bmatrix} \alpha_x \\ \alpha_y \\ \alpha_z \end{bmatrix} \\ &\triangleq \begin{bmatrix} n_1^T \\ n_2^T \end{bmatrix} \alpha \triangleq N\alpha. \end{aligned} \tag{28}$$

3. Optimal navigation star

Eq. (28) indicates that, when only the positioning and orientation errors are taken into account, it is the projection α_s of the vector formed by the misalignment angles in the subspace N_s spanned by n_1 and n_2 that affects the injection accuracy. Hence, according to Eq. (16), if the subspace $H_s = span\{h_1 h_2\}$ is designed to be equivalent to N_s by choosing the vectors h_1 and h_2 (basically the direction angles e_s and σ_s of the navigation star), then the output of the star sensor w contains all useful information. The star in the particular direction is the optimal navigation star.

Table 1
Guidance accuracy comparison.

		Analysis covariance		Monte Carlo sampling	
		Inertial	Integrated	Inertial	Integrated
Δa /m	Mean	0.0	0.0	55.809	−2.684
	MSE	1981.861	74.083	2012.739	73.558
Δi /deg	Mean	0.0	0.0	-3.857×10^{-3}	-1.394×10^{-3}
	MSE	1.067×10^{-1}	3.847×10^{-2}	1.092×10^{-1}	3.819×10^{-2}
$\Delta \Theta$ /deg	Mean	0.0	0.0	-3.607×10^{-4}	-1.984×10^{-4}
	MSE	1.272×10^{-2}	5.476×10^{-3}	1.296×10^{-2}	5.438×10^{-3}

We can derive $\boldsymbol{\alpha}_s$ from Eq. (16)

$$\boldsymbol{\alpha}_s = \boldsymbol{H}^T \left(\boldsymbol{H} \boldsymbol{H}^T \right)^{-1} \boldsymbol{w}. \tag{29}$$

Consequently, the correction equation is

$$\begin{bmatrix} \Delta m_{1s} \\ \Delta m_{2s} \end{bmatrix} = \boldsymbol{N} \boldsymbol{H}^T \left(\boldsymbol{H} \boldsymbol{H}^T \right)^{-1} \boldsymbol{w}. \tag{30}$$

The corrected injection parameters are $\Delta m_1 - \Delta m_{1s}$ and $\Delta m_2 - \Delta m_{2s}$. Because the orthogonal complement spaces of $\boldsymbol{N}_s$ and $\boldsymbol{H}_s$ should be equivalent, the optimal stellar direction can be obtained by solving

$$\boldsymbol{h}_1 \times \boldsymbol{h}_2 = \frac{\boldsymbol{n}_1 \times \boldsymbol{n}_2}{|\boldsymbol{n}_1 \times \boldsymbol{n}_2|}. \tag{31}$$

4. Numerical simulation analysis

In this section, numerical simulations conducted to evaluate the effect of the integrated guidance technique are presented. It is supposed that a Sun-synchronous satellite with an orbital altitude of 485 km is launched. The geographic coordinates of the launch point were set to 111.61°E, 38.85°N, and the launch azimuth A_0 was 192.94°. The positioning and orientation errors were assumed to have normal distributions with zero means, and the mean square errors (MSEs) were set as $\sigma_\Delta = [40'' \, 40'' \, 60'']^T$.

After some skipped calculations, the partial derivative matrix of the correction parameters with regard to the positioning and orientation errors was obtained

$$\begin{bmatrix} \partial a / \partial \boldsymbol{\Delta}^T \\ \partial i / \partial \boldsymbol{\Delta}^T \\ \partial \Theta_k / \partial \boldsymbol{\Delta}^T \end{bmatrix}$$

$$= \begin{bmatrix} 5.195 \times 10^6 & 8.720 \times 10^6 & 7.933 \times 10^5 \\ 4.083 \times 10^{-1} & 3.646 \times 10^{-1} & 6.700 \times 10^{-1} \\ 1.587 & 1.621 & 6.220 \end{bmatrix}.$$

A star in the direction of $e_s = 45°$ and $\sigma_s = 45°$ was adopted as the navigation star. The analysis covariance method and Monte Carlo sampling were employed to obtain the guidance accuracy for both the integrated and purely inertial guidance schemes. The number of samples was 400. Table 1 lists the results.

The results in Table 1 show the accordance of the results obtained using the two methods. By comparing the accuracy data of the two schemes, it is clear that both the correction schemes proposed above effectively improve the injection accuracy. When compared the results with the INS/GPS system, the stellar/inertial guidance system is less accurate. Navigation data compensation is only provided after cutoff, while the INS/GPS is available for all the boost phase. However, our intention is to propose an alternative that does not rely on any man-made signals and that can significantly improve the injection accuracy.

Figs. 3, 4, and 5 show the integrated guidance accuracies of the semi-major axis, orbital inclination, and flight path angle with regard to the direction of the navigation star, respectively. The results
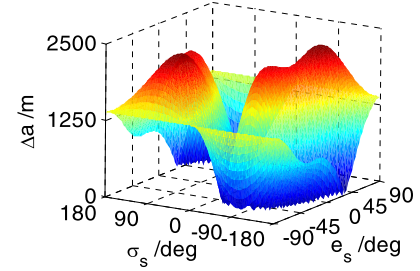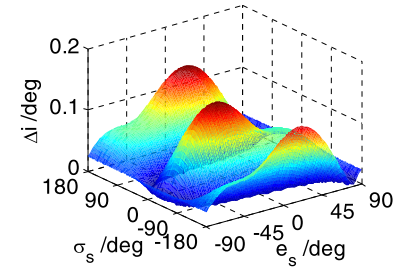

Fig. 3. Semi-major axis accuracy.

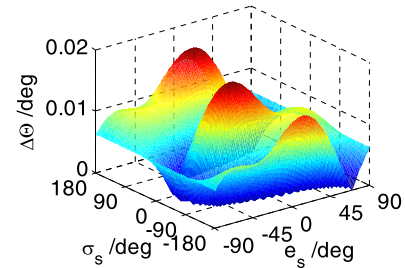
Fig. 4. Orbital inclination accuracy.

Fig. 5. Flight path angle accuracy.

reveal that the direction of the navigation star strongly affects the guidance accuracy.

When comparing the results presented in the figures and Table 1, it is found that the accuracy of integrated guidance is sometimes even poorer than that of the purely inertial guidance. The reason is that the correction coefficients used in the simulations are defined in Eq. (30) with regard to the optimal navigation star. When the adopted star considerably departs from the optimal one, the original inertial deviation may be overly corrected. To avoid this problem, different correction coefficients corresponding to the adopted stars should be used during simulations.

Fig. 6 consists of sections of Fig. 3. The plots show that two stars will have the same correction effects when they are collinear in terms of the origin of frame I; i.e., $e_{s1} = -e_{s2}$ and $|\sigma_{s1} - \sigma_{s2}| = \pi$.

Employing the method presented in Section 3, the optimal stellar direction was obtained. For the scheme using the semi-
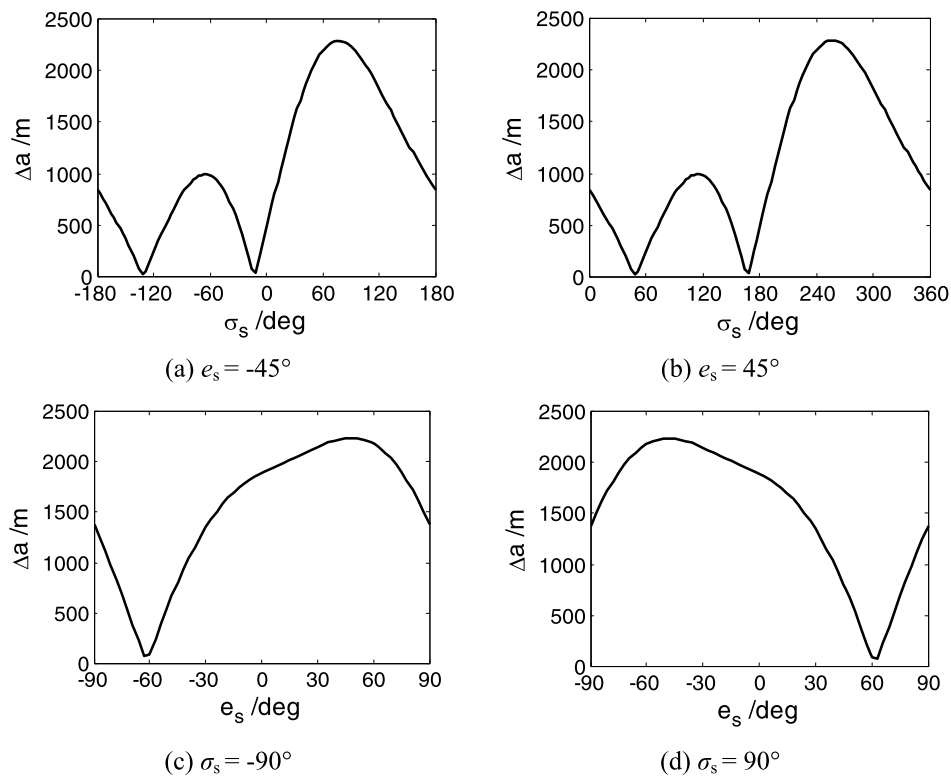
(a) $e_s = -45°$

(b) $e_s = 45°$

(c) $\sigma_s = -90°$

(d) $\sigma_s = 90°$

Fig. 6. Sections of semi-major accuracy.

major axis and the orbital inclination, the results are $e_{s\,opt\,1} = 60.920°$ and $\sigma_{s\,opt\,1} = 84.795°$. For the second scheme, the results are $e_{s\,opt\,2} = 37.393°$ and $\sigma_{s\,opt\,2} = 74.544°$. Computations show that the original inertial injection errors can be totally corrected through measurements of the optimal navigation star. Moreover, as mentioned above, the use of another star that is collinear with the optimal star in terms of the origin of frame I can achieve the same accuracy.

Employing the optimum correction method, more simulations were conducted accounting for all related errors. The results show that, when the optimal navigation star is adopted, the integrated guidance can remarkably improve the injection accuracy. If the semi-major axis and the inclination are corrected, the accuracies are approximately enhanced by 1.5 times and 5 times. In the second correction scheme, the accuracies of the inclination and flight path angle are approximately enhanced 4 times and 4.5 times.

5. Conclusions

Referring to the principles of stellar/inertial integrated guidance used for ballistic missiles, this paper studied the application of such guidance to responsive launch vehicles. Error transition and measurement equations were derived when only the positioning and orientation errors were taken into account. Two injection error correction schemes were proposed, and numerical analyses were conducted to evaluate the performance of the integrated guidance technique. Results show that the stellar/inertial guidance system is a suitable alternative for responsive space-lift.

Nevertheless, only the fundamentals of the approach are discussed here. The elements that affect the realization of an integrated guidance system are simplified, and the correcting procedure has not yet been implemented. Thus, many issues still require investigation.

References

[1] J. Ali, C.Y. Zhang, J.C. Fang, An algorithm for astro-inertial navigation using CCD star sensors, Aerospace Science and Technology 10 (2006) 449–454.

[2] I.Y. Bar-Itzhack, R.R. Harman, Optimized TRIAD algorithm for attitude determination, Journal of Guidance, Control, and Dynamics 20 (1) (1997) 208–211.

[3] V.A. Chobotov, Orbital Mechanics, third edition, AIAA Education Series, 2003, pp. 59–83.

[4] H.B. Christophersen, R.W. Pickell, J.C. Neidhoefer, et al., A compact guidance, navigation, and control system for unmanned aerial vehicles, Journal of Aerospace Computing, Information and Communication 3 (May 2006) 187–213.

[5] J.L. Crassidis, F.L. Markley, Unscented filtering for spacecraft attitude estimation, Journal of Guidance, Control, and Dynamics 26 (4) (2003) 536–542.

[6] Z.W. Fan, Current state of the development of star light inertial guidance technology and performance analysis, National Air Intelligence Center, ADA310487, May 1996.

[7] F. Gul, J.C. Fang, Alternate of GPS for ballistic vehicle navigation, in: Proceedings of IEEE Systems and Control in Aerospace and Astronautics, Jan. 2006, pp. 19–24.

[8] J.M. Hanson, M.W. Shrader, C.A. Cruzen, Ascent guidance comparisons, in: AIAA Guidance, Navigation, and Control Conference and Exhibit, AIAA, Scottsdale, AZ, 1–3 Aug. 1994.

[9] M. Idan, Estimation of Rodrigues parameters from vector observations, IEEE Transactions on Aerospace and Electronic Systems 32 (2) (1996) 578–585.

[10] D.F. Lawden, Optimal Trajectories for Space Navigation, Butterworths, London, 1963.

[11] J.M. Lorga, Q.P. Chuy, J.A. Mulder, et al., Evaluating the performance of an integrated navigation system, in: AIAA Guidance, Navigation, and Control Conference and Exhibit, San Francisco, CA, 15–18 Aug. 2005.

[12] P. Lu, B.F. Pan, Highly constrained optimal launch ascent guidance, Journal of Guidance, Control, and Dynamics 33 (2) (2010) 404–414.

[13] G.E. Mueller, D. Kohrs, R. Bailey, G. Lai, Autonomous safety and reliability features of the K-1 avionics system, Acta Astronautica 54 (2004) 363–370.

[14] M. Murphy, S. Armacost, R. Barnes, et al., Ballistic missile guidance system test in an aircraft pod, in: AIAA Guidance, Navigation, and Control Conference, Denver, CO, Aug. 2000.

[15] S.F. Rounds, G. Marmar, Stellar-inertial guidance capabilities for advanced ICBM, in: Guidance and Control Conference, Gatlinburg, TN, Aug. 15–17, 1983, pp. 849–855.

[16] J.H. Saleh, G.F. Dubos, Responsive space: Concept analysis and theoretical framework, Acta Astronautica 65 (2009) 376–398.

[17] G.T. Schmidt, INS/GPS technology trends, in: NATO RTO Lecture Series SET-116, Low-Cost Navigation Sensors and Integration Technology, March 2010, pp. 1-1–1-22.

[18] S. Theil, S. Steffes, M. Samaan, M. Conradt, Hybrid navigation system for space-planes, launch and re-entry vehicles, in: Proceedings of 16th AIAA/DLR/DGLR International Space Planes and Hypersonic Systems and Technologies Conference, Bremen, Germany, Oct. 19–22, 2009.

[19] J.F. Vasconcelos, P. Oliveira, C. Silvestre, Inertial navigation system aided by GPS and selective frequency contents of vector measurements, in: AIAA Guidance, Navigation, and Control Conference and Exhibit, San Francisco, CA, 15–18 Aug. 2005.

[20] M.J. Veth, J.F. Raquet, Alignment and calibration of optical and inertial sensors using stellar observations, in: Proceedings of ION GNSS 2005, Sep. 2005, pp. 2494–2503.

[21] G. Wahba, A least squares estimate of spacecraft attitude, SIAM Review 7 (3) (1965) 409.

[22] J. Wang, J. Chun, Attitude determination using a single-star sensor and a star-density table, Journal of Guidance, Control, and Dynamics 29 (6) (2006) 1329–1338.

[23] S.P. Worden, R.R. Correll, Responsive space and strategic information, Defense Horizons 40 (April 2004) 1–8.

[24] A.D. Wu, E.N. Johnson, A.A. Proctor, Vision-aided inertial navigation for flight control, Journal of Aerospace Computing, Information and Communication 2 (September 2005) 348–360.

[25] L.J. Zhang, H.S. Sun, Ascent guidance for responsive launch: a fixed-point approach, in: AIAA Guidance, Navigation, and Control Conference and Exhibit, San Francisco, CA, 15–18 Aug. 2005.